AUTHOR QUERY FORM

ELSEVIER	**Journal:** PRP **Article Number:** 50865	**Please e-mail or fax your responses and any corrections to:** **E-mail:** corrections.esch@elsevier.thomsondigital.com **Fax:** +353 6170 9272

Dear Author,

Please check your proof carefully and mark all corrections at the appropriate place in the proof (e.g., by using on-screen annotation in the PDF file) or compile them in a separate list. Note: if you opt to annotate the file with software other than Adobe Reader then please also highlight the appropriate place in the PDF file. To ensure fast publication of your paper please return your corrections within 48 hours.

For correction or revision of any artwork, please consult http://www.elsevier.com/artworkinstructions.

Any queries or remarks that have arisen during the processing of your manuscript are listed below and highlighted by flags in the proof. Click on the 'Q' link to go to the location in the proof.

Location in article	Query / Remark: click on the Q link to go Please insert your reply or correction at the corresponding line in the proof
	Reference(s) given here were noted in the reference list but are missing from the text – please position each reference in the text or delete it from the list.
Q1	Please confirm that given names and surnames have been identified correctly.
Q2	The country name has been inserted for the affiliations 'a' and 'b'. Please check, and correct if necessary.
Q3	Please check the hierarchy of the section headings.
Q4	Uncited reference: This section comprises reference that occurs in the reference list but not in the body of the text. Please position the reference in the text or, alternatively, delete it. Any reference not dealt with will be retained in this section.

Thank you for your assistance.

Pathology – Research and Practice xxx (2012) xxx–xxx

Contents lists available at SciVerse ScienceDirect

Pathology – Research and Practice

journal homepage: www.elsevier.de/prp

Short communication

Morphometric analysis of hepatocellular nodular lesions in HCV cirrhosis

Maurizio Vertemati[a,*], Claudia Moscheni[b], Duccio Petrella[c], Luca Lamperti[b], Mara Cossa[b], Marcello Gambacorta[c], Maria Goffredi[b], Laura Vizzotto[b]

[a] Dipartimento di Morfologia Umana e Scienze Biomediche "Città Studi", Faculty of Pharmacy, University of Milan, Italy
[b] Dipartimento di Morfologia Umana e Scienze Biomediche "Città Studi", Faculty of Medicine, University of Milan, Italy
[c] Department of Pathology, Niguarda Hospital, Milan, Italy

ARTICLE INFO

Article history:
Received 23 June 2011
Received in revised form 2 February 2012
Accepted 15 February 2012

Keywords:
Morphometry
Hepatic nodules
Cirrhosis
Immunohistochemistry

ABSTRACT

We generated a computerized morphometric model to evaluate and quantify the morphological features in large regenerative nodules (LRN), high-grade dysplastic nodules (HGDN) and hepatocellular carcinoma (HCC).

Sixteen LRN, 10 HGDN and 16 HCC in HCV-cirrhotic livers were stained with H&E, smooth muscle actin, CD34, CD31 and reticulin to evaluate volume and surface fractions.

On H&E stains, the most discriminatory features between LRN, HGDN and HCC were volume fraction and the number of hepatocyte nuclei in unit volume and hepatocyte nuclear/cytoplasmic ratio. On immunohistochemistry, volume fractions of capillarised sinusoids, capillary units and isolated arteries were significantly different among all groups and highest in HCC; surface fraction of reticulin was markedly decreased in HCC.

Our morphometric model is an objective method for quantification of the morphological changes of the nodular lesions, and it could be applied to studies involving histological evaluation of the spectrum of nodular lesions arising in the cirrhotic liver.

Introduction

Hepatocarcinogenesis is considered a multistep process with accumulation of genetic and epigenetic alterations evolving from normal through cirrhosis and dysplastic nodules to hepatocellular carcinoma (HCC) [4]. Increased cell proliferation and mitotic-associated genes are generally involved in hepatocarcinogenesis [19].

The terminology of nodular lesions in cirrhotic liver has become well established since the International Working Party Classification (IWP) in 1995 [6]. Nodules are classified as large regenerative nodules (LRN), as multiacinar regenerative nodules that are distinctly larger (i.e. >5 mm) than the background of cirrhotic nodules, and dysplastic nodules that are defined as nodules of hepatocytes with dysplasia but without definite histological criteria of malignancy; based on cellular architecture, degree of dysplasia, presence or absence of portal tracts and cytological features. Dysplastic nodules are subdivided into low-grade nodules that do not have any cytological or architectural atypia to suggest emerging HCC, and high-grade dysplastic nodules that show a thick cell plate and occasional pseudoglandular structures and nontriadal arteries [1,6,14].

Tumor angiogenesis is one of the fundamental requirements for tumor growth and proliferation [12]. The infiltrating inflammatory cells in tumor are closely related to tumor angiogenesis, and this could be the consequence of the production of cell factors and enzymes which participate in the growth and spread of tumors [13].

Diagnosis of focal hepatocellular lesions is still a complex issue: moreover, histology-based diagnosis of HCC may also suffer from a moment of subjectivity due to inter- and intraindividual variations during semiquantitative analysis. Immunohistochemistry has furnished a panel of markers to analyze the differences in the angioarchitecture of the nodular lesions in the cirrhotic liver (i.e. large regenerative nodules, dysplastic nodules and HCC): CD31 to detect capillary units, CD34 to evaluate capillarised sinusoids and smooth muscle alpha actin (SMA) to detect unpaired arteries [2,5,7].

Our aim was to apply a computerized morphometric model to evaluate and quantify the morphological features in LRN, high-grade dysplastic nodules (HGDN) and HCC in HCV-related cirrhosis.

Materials and methods

We studied 16 LRN (median size = 7 mm, range 5–14 mm), 10 HGDN (median size = 11 mm, range 7–18 mm), 16 HCC (median size = 25 mm, range 22–31 mm), and 25 cirrhotic nodules (CN) (median size = 3 mm, range 2–4 mm) surrounding the mentioned

* Corresponding author at: Dept. of Morfologia Umana e Scienze Biomediche Città Studi, Via Mangiagalli, 31, 20133 Milan, Italy. Tel.: +39 0250319662.
E-mail address: maurizio.vertemati@unimi.it (M. Vertemati).

0344-0338/$ – see front matter © 2012 Published by Elsevier GmbH.
doi:10.1016/j.prp.2012.02.007

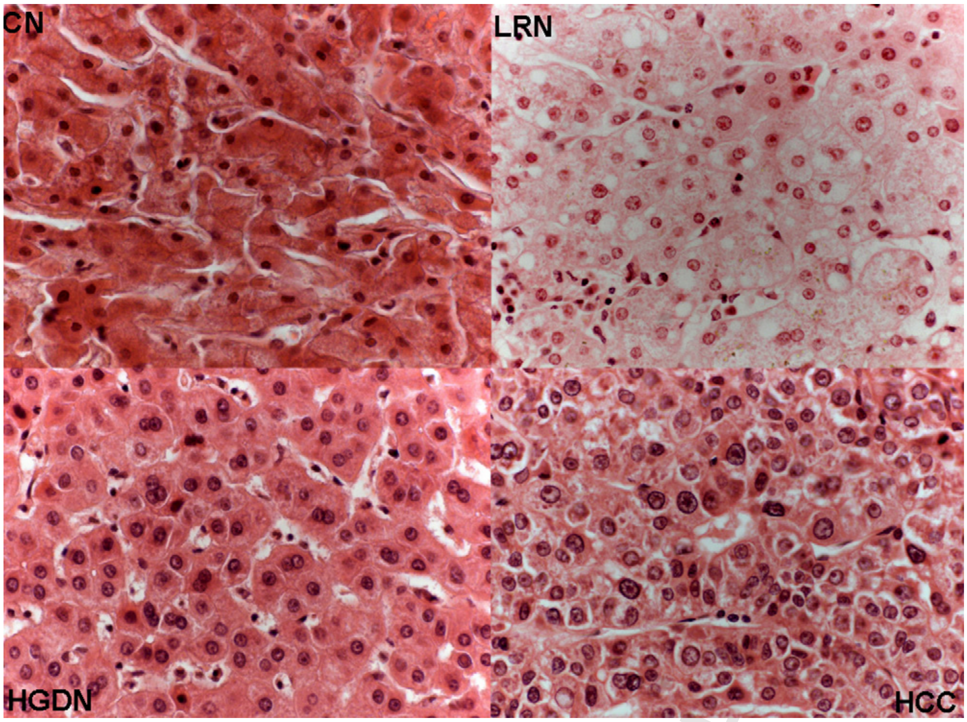

Fig. 1. Composite of H&E-stained tissue sections (40× magnification) for each nodular lesion.

lesions were the control group. Specimens from excised liver were obtained from the archival files of 42 patients (32M/10F) submitted to liver transplantation at Niguarda Hospital Milan for HCV-related cirrhosis. All specimens were examined by two pathologists, and a consensus determination was made following the criteria and the nomenclature of the IWP [6].

HGDN showed at least moderate cytological or architectural atypia, increased cell density, more than 2 times higher than that of the adjacent liver tissue, and small-cell change (i.e. hepatocytes showing decreased cell volume, increased nuclear/cytoplasmic ratio, mild nuclear pleomorphism, giving the impression of nuclear crowding).

According to our standard operating procedure for routine histological diagnosis, livers removed at transplantation are delivered immediately to our laboratory where they are examined and fixed promptly. This procedure allows proper fixation, including focal lesions, and reduces artifacts due to delayed fixation, which may affect the histological interpretation and morphometric analysis.

The research protocol was approved by the institutional review boards.

In all cases investigated, some 2-cm^3 blocks were obtained from the excised liver, then formalin fixed soon after the receipt of the liver specimen and embedded in paraffin. For each case, 5 consecutive sections (4 μm) were obtained from the selected block.

Each section series was stained as follows:

- Hematoxylin–eosin (HE) to assess volume fractions of parenchymal and extraparencymal compartments; Fig. 1 shows one histological example of each type of lesion stained by HE (40× magnification).
- Monoclonal antibodies against: (a) cell surface antigen CD31 to evaluate CD31-immunoreactive microvessels, (b) SMA to assess the number of unpaired arterioles, (c) CD34 to evaluate sinusoidal capillarisation.
- Silver impregnation for reticulin fibers to evaluate hepatic cell plate architecture.

The morphometric model for liver characterization consisted of many stereological variables [17,18].

All morphometric variables were obtained using a computerized image analyzer (Kontron-Zeiss KS400). To examine the microscopic fields, two objectives, 10× and 40×, were used.

The stepping procedure was controlled automatically to assure unbiased sampling, and more than 400 microscopic fields systematically selected were examined.

The observer can interactively apply techniques of enhancement for a better definition of parenchymal and vascular structures. Fields not suitable for analysis due to technical artifacts can be excluded. An algorithm automatically controls the scanning stage operation in order to avoid duplicate measurements of the same structures.

Volumetric analysis was carried out by a differential point-counting procedure on different grids of points that were automatically overlaid onto each microscopic field (at 40× magnification) displayed on the monitor. A 16-points square lattice was used to evaluate parenchymal and extraparenchymal components (i.e. hepatocytes, sinusoids, sinusoids-like blood spaces and fibrosis) and a 144-points square lattice to evaluate hepatocyte nuclei and cytoplasm, portal triads, centrilobular veins and immunohistochemical variables (CD31, CD34 and SMA).

Both grids were automatically overlaid onto each microscopic field displayed on the monitor. Each point was classified as overlying the reference structures of interest on all sections [3].

Surface area of reticulin was evaluated on sections at 10× magnification by superimposing on each microscopic field a grid of four lines; surface densities were calculated by differential intersection counting [10].

The number in unit volume was derived by diameter analysis following the Schwartz–Saltykov method [15].

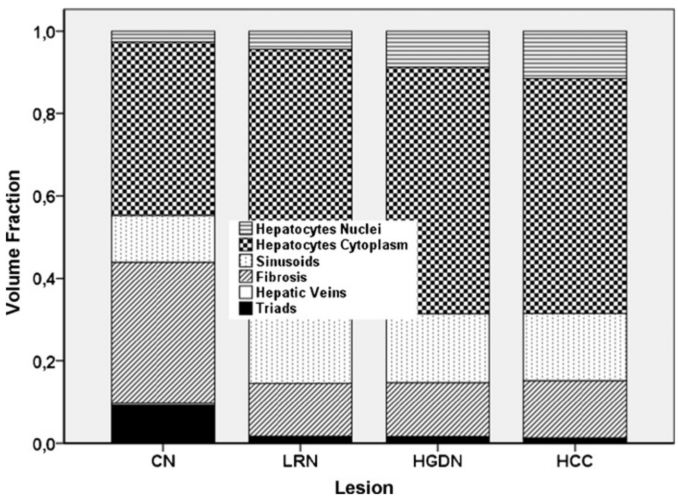

Fig. 2. Percentage of the different subcomponents relative to parenchymal (hepatocellular and sinusoids) and extraparenchymal (portal triads, fibrosis and centrilobular veins) compartments of nodular lesions evaluated on HE stain. All nodular lesions investigated are characterized from a severe disruption of the vascular architecture, and the term centrilobular veins is referred to the central veins involved in the fibrotic process.

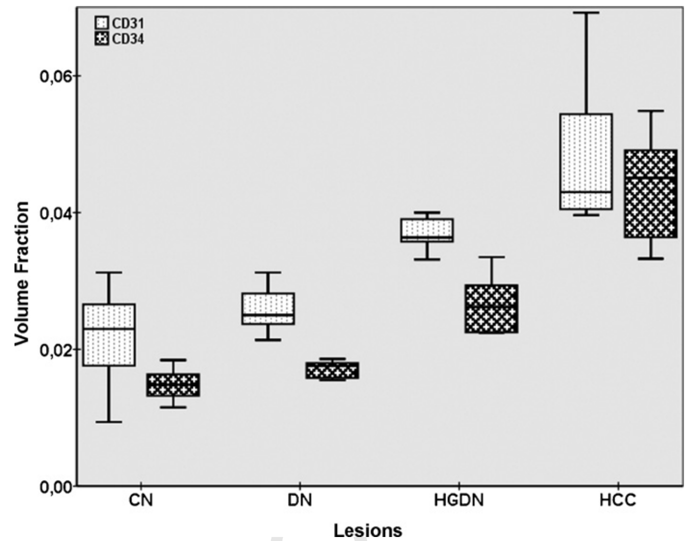

Fig. 3. CD31 and CD34 volume fractions in the nodular lesions (LRN, HGDN and HCC) and in the perilesional cirrhotic nodules (CN). For CD31 immunostaining, vessels in the fibrous septa or in the capsule of the nodule were excluded from counting.

During point counting procedure, an experienced operator blinded to the pathologist's diagnosis or clinical history identified the different structures. Moreover, to assess the reproducibility of our morphometric model, 10 specimens were randomly selected from the entire pool of biopsies, reassessed as above by another blinded operator and compared with the initial counting.

Statistical analysis

SPSS 17.1 software was used for statistical analysis. For each parameter, a comparison among different groups was performed by variance analysis with factorial design followed by Scheffe's post hoc test. Furthermore, variance analysis was used to test the reproducibility of the morphometric analysis, according to the results obtained by two blinded operators.

Results

Results are shown in Tables 1–3, and in Figs. 2–5.

On HE-stained sections, the number of nuclei hepatocytes in unit volume showed the highest values in HGDN and HCCs (CN 205,785, LRN 140,344, HGDN 374,629, HCC 394,622). Conversely,

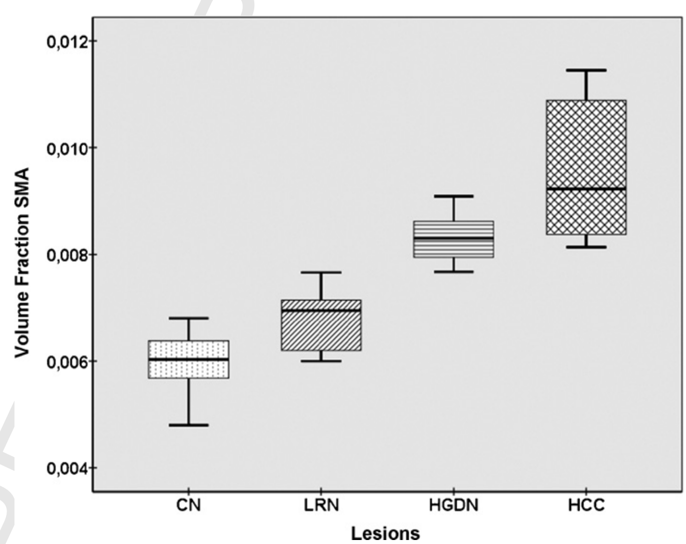

Fig. 4. SMA volume fraction in the nodular lesions (LRN, HGDN and HCC) and in the perilesional cirrhotic nodules (CN).

Table 1
Main morphometric variables evaluated for the different nodular lesions (means ± standard deviations)*. *p* Values = probability values in ANOVA (source between pathologies). Equal symbols mark homogeneous subsets in Scheffè post hoc test.

	Dimension	CN	LRN	HGDN	HCC	*p* Values
$V_v$cit	mm^3/mm^3	.4472 ± .0892	.6966 ± .0343°	.6861 ± .0475°	.6853 ± .0595°	<.001
$V_v$nuc	mm^3/mm^3	.0274 ± .0065*	.0445 ± .0072°	.0877 ± .0126◊	.1150 ± .0051■	<.001
$V_v$sinend	mm^3/mm^3	.1141 ± .0397	.1581 ± .0440°	.1672 ± .0242°	.1633 ± .0295°	<.001
$V_v$cenlo	mm^3/mm^3	.0049 ± .0067	.0023 ± .0046	.0010 ± .0022	.0008 ± .0020	.239
$V_v$fib	mm^3/mm^3	.3421 ± .0954	.1286 ± .0094°	.1310 ± .0363°	.1391 ± .0696°	<.001
$V_v$tria	mm^3/mm^3	.0916 ± .0444	.0145 ± .0086°	.0147 ± .0066°	.0078 ± .0098■	<.001
N/C	–	.062 ± .012*	.064 ± .013*	.128 ± .021°	.169 ± .023■	<.001
N_V	$1/mm^3$	205,488 ± 114,745*	140,344 ± 55,427*	374,630 ± 87,194■	394,622 ± 287,757■	<.001
$\bar{d}_{nuc}$	μm	7.89 ± .81	7.89 ± .41	8.30 ± .68	8.83 ± .67	.516
$\bar{V}$	μm^3	2872.75 ± 1629.43*	5839.61 ± 2574.52	1937.30 ± 558.24*	2433.55 ± 1233.52*	<.001
$\bar{d}_{hep}$	μm	17.029 ± 3.227*	21.855 ± 3.309	15.322 ± 1.423*	16.18 ± 3.17*	<.001

Volume fractions in the test area = 504 × 504 pixels occupied by hepatocyte nuclei ($V_v$nuc), hepatocyte cytoplasm ($V_v$cit), sinusoids (lumen and endothelium – $V_v$sinend), fibrosis ($V_v$fib), centrilobular veins ($V_v$cenlo), portal triads (hepatic arteries, portal veins and biliary ducts – $V_v$tria), number in unit volume and size distribution of hepatocyte nuclei (N_V), mean hepatocyte diameter ($\bar{d}_{hep}$) and volume ($\bar{V}$). $\bar{V}$ was calculated by dividing the hepatocyte volume fraction ($V_v$cyt + $V_v$nuc) by N_V; $\bar{d}_{hep}$ was then calculated as the diameter of a sphere of volume $\bar{V}$.

Please cite this article in press as: M. Vertemati, et al., Morphometric analysis of hepatocellular nodular lesions in HCV cirrhosis, Pathol. – Res. Pract (2012), doi:10.1016/j.prp.2012.02.007

Table 2
Morphometric variables evaluated by immunostaining for the different nodular lesions (means ± standard deviations are quoted). *p* Values = probability values in ANOVA (source between pathologies). Equal symbols mark homogeneous subsets in Scheffè post hoc test.

Marker	Dimension	CN	LRNs	DN	HCC	*p* Values
CD31	mm^3/mm^3	.0219 ± .0060*	.0258 ± .0035*	.0368 ± .0025°	.0481 ± .0105^	<.001
CD34	mm^3/mm^3	.0149 ± .0021*	.0171 ± .0012*	.0267 ± .0043°	.0436 ± .0077^	<.001
SMA	mm^3/mm^3	.0060 ± .0006*	.0067 ± .0006*	.0083 ± .0005°	.0096 ± .0014^	<.001
Ret	mm^2/mm^3	29.018 ± 7.631*	29.964 ± 1.553*	19.777 ± 2.245°	11.964 ± 2.394^	<.001

Volume fractions occupied by CD31 immunoreactive vessels ($V_v$cpu), capillarised sinusoids (V_vCD34), individual lesional arteries (alpha-SMA-positive arterioles) and surface fractions occupied by reticulin (S_vRet).

Table 3
Statistical analysis of inter-observer agreement on morphometric analysis: 10 randomly selected specimens are compared with initial point counting. *F* represents the variance ratio related to the source of error for each evaluation by the two operators; df(1,67).

	$V_v$cit	$V_v$nuc	$V_v$sinend	$V_v$cenlo	$V_v$fib	$V_v$tria	CD31	CD34	SMA	Ret
F	0.739	0.459	0.087	0.401	0.059	0.957	0.972	0.045	0.058	0.912
p	0.478	0.747	0.858	0.664	0.631	0.298	0.429	0.867	0.789	0.364

the mean hepatocyte volume was significantly higher in LRN. The nuclear/cytoplasmic ratio was highest in HCC (CN .062, LRN .064, HGDN .128, HCC .169). The volume fractions of centrilobular veins, sinusoids and fibrosis did not differ among the different nodular lesions. The volume fraction of portal triads was lowest in HCC, where they may represent portal tracts entrapped by infiltrating tumor [6].

The number of hepatocytes in unit volume (N_V) showed the highest values in HCC and HGDN when compared to LRN and CN. It must be underlined that the nuclear measurements do not take into account distortion related to sections thickness [8]. Moreover, due to the overlap in values between the different categories, the interpretation of these parameters is difficult. The nuclear/cytoplasmic ratio was highest in HCC.

On immunohistochemical stains (Table 2), volume fractions of CD31-immunoreactive microvessels ($V_v$cpu: CN .219, LRN .258, HGDN .368, HCC .481), of capillarised sinusoids (V_vCD34: CN .149, LRN .171, HGDN .267, HCC .436) and of unpaired arterioles (SMA: CN .0060, LRN .0067, HGDN .0083, HCC .0096) were highest in HCC. Conversely, the surface fraction of reticulin was highest in LRN and CN, and lowest in HCC (S_vRet: CN 29.02, LRN 29.9, HGDN 19.8, HCC 11.9).

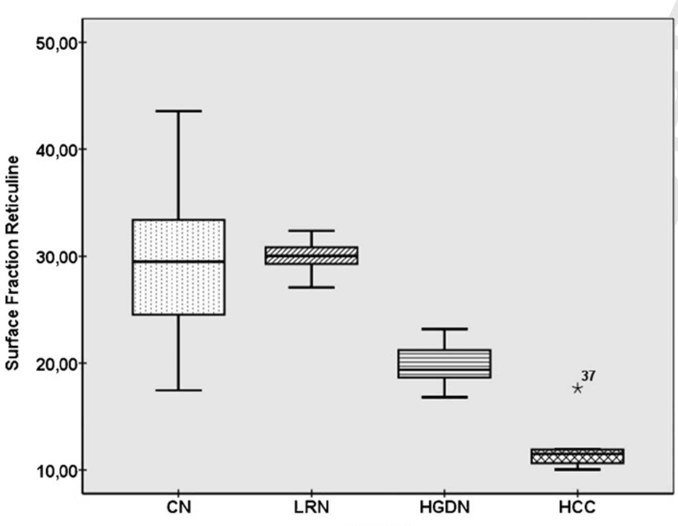

Fig. 5. Reticuline surface fraction in the nodular lesions (LRN, HGDN and HCC) and in the perilesional cirrhotic nodules (CN). The symbol *37 shows that one HCC has a surface fraction of reticuline well away, i.e. more than 3 times the 75–25 interquartile distance from the rest of the tumors.

Fig. 2 shows the percentage of parenchymal (hepatocellular and sinusoids) and extraparenchymal (portal triads, fibrosis and centrilobular veins) components relative to all hepatocellular nodular lesions evaluated on HE stain.

Figs. 3–5 show, respectively, the volume fractions referred to immunohistochemical staining for each lesion investigated.

Table 3 shows high inter-observer agreement in assessing the morphometric characteristics of the lesions.

Table 4 shows the average and upper or lower deviation standard of some morphometric parameters that are more discriminated among the nodular lesions.

Discussion

Hepatocellular carcinoma develops via a progressive pathway from premalignant nodular lesions to HCC in the cirrhotic liver. However, differentiating a premalignant lesion from HCC is often difficult [6,8]. In this “technical” paper, we used a morphometric approach to evaluate and quantify the morphological features in LRN, HGDN and HCC in HCV-related cirrhosis.

On HE stains, when considering the parenchymal compartment (Table 1 and Fig. 1), the most intriguing results were related to the hepatocyte compartment that showed significantly higher volume fractions of hepatocyte nuclei ($V_v$nuc) in HCC, while the volume fraction of hepatocyte cytoplasm ($V_v$cit) was similarly significantly higher in HCC, HGDN and LRN. Of note, the number of hepatocytes in unit volume (N_V) showed the highest values in HCC and HGDN (with the most extensive increase in HCC), where cell density is

Table 4
Morphometric values expressed in terms of average values and standard deviation that are more discriminating among nodular lesions.

Marker	LRNs	HGDN	HCC
$V_v$nuc	<.0512	.1003–.0651	>.1099
N/C	<.077	.149–.107	>.146
CD31	<.0293	.0393–.0343	>.0376
CD34	<.0183	.0310–.0224	>.0359
SMA	<.0073	.0088–.0078	>.0082
Ret	>28.41	22.02–17.53	<14.36

The column referred to LRNs shows the values related to the average and upper deviation standard ($V_v$nuc, N/C, CD31, CD34, SMA) and to the average and lower deviation standard for reticulin evaluated by morphometry for the parameters that, according to our data, discriminate among the different lesions investigated; in the column referred to HGDN are shown respectively the values of the average and upper deviation standard and of the average and lower deviation standard; in the column of HCC are reported the values of the average and lower deviation standard.

Please cite this article in press as: M. Vertemati, et al., Morphometric analysis of hepatocellular nodular lesions in HCV cirrhosis, Pathol. – Res. Pract (2012), doi:10.1016/j.prp.2012.02.007

1.5–2 higher than in LRN. Conversely, the mean hepatocyte volume was highest in LRN.

The nuclear/cytoplasmic ratio progressively increased in HGDN and HCC, with the highest values in HCC, while CN and LRN showed similar values.

According to these results, it could be resumed that HCC and HGDN are characterized by increased nuclear and cellular density, which appear as "nuclear clouding" in histological specimens, when compared to LRN.

In this context, only a morphometric evaluation can objectively evaluate and give evidence of such differences and assign them statistical significance.

When considering immunohistochemical analysis (Table 3), the volume fractions occupied by CD31-immunoreactive microvessels and capillarised sinusoids (Fig. 3) and individual lesional arteries (Fig. 4) were highest in HGDN and HCC (with the most extensive increase in HCC) [9,11].

Lastly, when compared to LRN, the surface fraction of reticulin (Fig. 5) was markedly reduced in HGDN and HCC (with the lowest values in HCC).

The increased cell density with increased N/C ratio, the different vascular profile (i.e. sinusoidal capillarisation and unpaired arteries) and the decrease/loss of reticulin in hepatocellular non-malignant and malignant nodules in the cirrhotic liver support the concept that HGDN represents a step toward neoplastic transformation.

Lastly, when considering CN and LRN, they showed a similar trend, suggesting that LRN are not dysplastic lesions.

To evaluate the reproducibility of our morphometric model, 10 randomly selected specimens were analyzed in a blinded fashion by another operator and compared with the results of the initial counting. As shown in Table 3, the agreement between the two morphometric evaluations was very high, underlying the reproducibility of our method.

Certainly, our morphometric model introduces numerical values and not just semiquantitative categories which, in future studies, could help identify subpopulations of HCC depending on their morphometric characteristics (as evidenced by the outlier in Fig. 4).

According to our data, we identified some parameters (Table 4) that could help to make the correct diagnosis and that could be coupled to and integrated in the classical microscopic pathology assessment (vascular and/or capsular invasion, necrosis, cellular atypia, mitosis) to conceivably enhance the reliability and uniformity of the diagnostic evaluation of hepatic nodular lesions.

Our computerized morphometric model, incorporating measures of the extremes of the cirrhosis to HCC spectrum, also considering LRN and HGDN categories, is simple and lacks observer or subjective bias and can be used to supplement objective methods to achieve precise and reader-independent quantification of the morphological characteristics of hepatocellular nodular lesions.

Further studies are needed to determine the role of our morphometric model for identifying subpopulations of HCC depending on their morphometric characteristics with a prospective cohort.

Uncited reference Q4

[16].

References

[1] M. Borzio, S. Bruno, M. Roncalli, C. Mels, G. Ramela, F. Borio, G. Leandro, E. Servida, M. Podda, Liver cell dysplasia is a major risk factor for hepatocellular carcinoma in cirrhosis: a prospective study, Gastroenterology 108 (3) (1995) 812–817.

[2] H.M. DeLisser, M. Christofidou-Solomidou, R.M. Strieter, M.D. Burdick, C.S. Robinson, R.S. Wexler, J.S. Kerr, C. Garlanda, J.R. Merwin, J.A. Madri, S.M.I. Albelda, Involvement of endothelial PECAM-1/CD31 in angiogenesis, Am. J. Pathol. 151 (1977) 671–677.

[3] H. Elias, A. Henning, D.E. Schwartz:, Stereology: applications to biomedical research, Physiol. Rev. 51 (1971) 158–200.

[4] P. Hytiroglou, Y.N. Park, G. Krinsky, N.D. Theise, Hepatic precancerous lesions and small hepatocellular carcinoma, Gastroenterol. Clin. N. Am. 36 (2007) 867–887.

[5] K. Ikeda, M. Kobayashi, S. Saitoh, T. Someya, T. Hosaka, H. Sezaki, Y. Suzuki, E. Suzuki, N. Akuta, Y. Arase, H. Kumada, Origin of neovascular structure in an early stage of hepatocellular carcinoma: study of alpha-smooth muscle actin immunohistochemistry in serial thin sections of surgically resected cancer, J. Gastroenterol. Hepatol. 21 (2006) 183–190.

[6] International Consensus Group for Hepatocellular Neoplasia, The international consensus group for hepatocellular neoplasia, Hepatology 49 (2) (2009) 658–664.

[7] D.S. Krause, M.J. Fackler, C.I. Civin, W.S. May, CD34: structure, biology and clinical utility, Blood 87 (1) (1996) 1–13.

[8] L. Libbrecht, V. Desmet, T. Roskams, Preneoplastic lesions in human hepatocarcinogenesis, Liver Int. 25 (2005) 16–27.

[9] L. Messerini, L. Novelli, C.E. Comin, Microvessel density and clinicopathological characteristics in hepatitis C virus and hepatitis B virus related hepatocellular carcinoma, J. Clin. Pathol. 57 (2004) 867–871.

[10] P.R. Mouton:, Principles and Practices of Unbiased Stereology, The Johns Hopkins University Press, Baltimore, London, 2002.

[11] Y. Nakashima, O. Nakashima, C.C. Hsia, M. Kojiro, E. Tabor, Vascularization of small hepatocellular carcinomas: correlation with differentiation, Liver 19 (1999) 12–18.

[12] Y.N. Park, Y.B. Kim, K.M. Yang, C. Park, Increased expression of vascular endothelial growth factor and angiogenesis in the early stage of multistep hepatocarcinogenesis, Arch. Pathol. Lab. Med. 124 (2000) 1061–1065.

[13] S. Peng, H. Deng, J.F. Yang, P.P. Xie, C. Li, H. Li, De-Y. Feng, Significance and relationship between infiltrating inflammatory cell and tumor angiogenesis in hepatocellular carcinoma tissues, World J. Gastroenterol. 11 (41) (2005) 6521–6524.

[14] M. Roncalli, Hepatocellular nodules in cirrhosis: focus on diagnostic criteria on liver biopsy. A Western experience, Liver Transpl. 10 (2004) S9–S15.

[15] S.A. Saltykov, A stereological method for measuring the specific surface area in metallic powders, in: H. Elias (Ed.), Proceedings of the Second International Congress for Stereology, Springer-Verlag, Berlin, 1967, pp. 63–64.

[16] N.D. Theise, Y.N. Park, M. Kojiro, Dysplastic nodules and hepatocarcinogenesis, Clin. Liver Dis. 6 (2) (2002) 497–512.

[17] M. Vertemati, E. Minola, M. Goffredi, G. Sabatella, M. Gambacorta, L. Vizzotto, Computerized morphometry of the cirrhotic liver: comparative analysis in primary biliary cirrhosis, alcoholic cirrhosis and posthepatitic cirrhosis, Microsc. Res. Tech. 65 (3) (2004) 113–121.

[18] M. Vertemati, L. Vizzotto, C. Moscheni, A. Dhillon, A. Dhillon, A. Quaglia, A morphometric model to minimize subjectivity in the histological assessment of hepatocellular carcinoma and its precursors in cirrhosis, Microsc. Res. Tech. 71 (8) (2008) 606–613.

[19] C.W. Wong, I.O.L. Ng, Molecular pathogenesis of hepatocellular carcinoma, Liver Int. 28 (2) (2007) 160–174.